Supplementary information for

Dual-role iron catalyst for covalent triazine framework synthesis and efficient CO_2 cycloaddition under mild conditions

Mozhdeh Pourmansouri,[a] Negin Amiraslani,[a] Piero Mastrorilli,[b] Stefano Todisco[b] and Mojtaba Khorasani*[a,c]

a) Department of Chemistry, Institute for Advanced Studies in Basic Sciences (IASBS), Zanjan 45137-66731, Iran. E-mail: m_khorasani@iasbs.ac.ir, Fax: +98-24-33153232; Tel: +98-24-3315-3223.

b) DICATECh Department, Politechnic of Bari, via Orabona, 4 70125 Bari, Italy

c) Research Center for Basic Sciences & Modern Technologies (RBST), Institute for Advanced Studies in Basic Sciences, IASBS, Zanjan 45137-66731, Iran.

Table of Contents

1. Materials and methods

1.1. Characterization

The particle morphology of the prepared materials was monitored by scanning electron microscope (SEM, TESCAN MIRA3 FE-SEM). Elemental mapping results were obtained by an energy dispersive spectrometer (EDS) attached to the SEM apparatus. N_2 adsorption isotherms were measured at 77 K by Belsorp (BELMAX, Japan) analyzer where samples were first pretreated at 353 K for 5 h. The specific surface area (S_{BET}) was determined from the linear part of the BET plot ($P/P_0 \approx 0.05$-0.15). Pore size distribution (D_{BJH}) was estimated from the BJH method from the adsorption branch of the isotherm. Total pore volume (V_t) was calculated from the amount of adsorbed nitrogen at a relative pressure of 0.99. Thermogravimetric analysis was performed by using a NETZSCH STA 409 PC/PG instrument at scan rates of 20 K min^{-1}, with typically about 5 mg sample under flowing N_2. Solid State NMR experiments were performed on a Bruker Avance I 400 spectrometer (^{13}C, 100.6 MHz) using a 4.0 mm HX MAS probe at 298 K. FT-IR spectra were recorded on a Brüker EQUINOX-55 instrument equipped with a liquid N_2-cooled MCT detector. X-ray photoelectron spectroscopy, XPS [BESTEC (EA 10)] determined the oxidation state of surface elements in the catalyst. Gas chromatography analyses were performed on Varian CP-3800 using a flame ionization detector (FID) using trimethylbenzene (TMB) as suitable internal standards. NMR spectra were recorded using a Brüker (^1H frequency: 400 MHz).

1.2. Synthesis

1.2.1. Synthesis of pyridine 2,6-dicarbonyl chloride

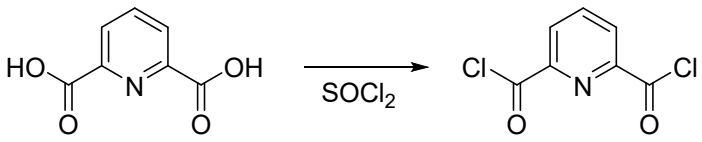

Pre-dried dipicolinic acid (4.00 g, 24 mmol) and thionyl chloride (40 mL, 550 mmol) were added to an oven-dried round-bottom Schlenk flask and refluxed under argon for 15 h. After cooling to ambient temperature, the excess thionyl chloride was removed under reduced pressure. The resulting solid was further dried in a vacuum oven overnight to afford pyridine-2,6-dicarbonyl chloride as a white powder (4.56, 93%).

1.2.2. Synthesis of dimethyl pyridine-2,6-dicarboxylate

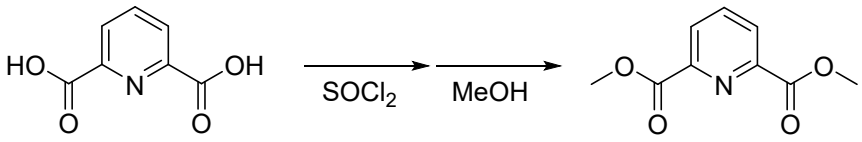

To a single-neck round-bottom flask containing pyridine-2,6-dicarboxylic acid (4.00 g, 24 mmol), $SOCl_2$ (30 mL, 414 mmol) was added dropwise at 0 °C. The reaction mixture was then refluxed for 12 h, followed by the slow addition of dry methanol (30 mL) at 0 °C (Caution: HCl(g) generates). The mixture was refluxed for a further 12 h. Excess $SOCl_2$ and MeOH were removed by distillation. Saturated $NaHCO_3$ solution (90 mg mL^{-1}) was added to the residue and the mixture was stirred for 30 min. The product was extracted with dichloromethane, and the combined organic layers were dried over anhydrous Na_2SO_4. Removal of the solvent afforded dimethyl pyridine-2,6-dicarboxylate as a white solid (4.2 g, 84%).

1.2.3. Synthesis of N^2,N^6-diphenylpyridine-2,6-dicarboxamide

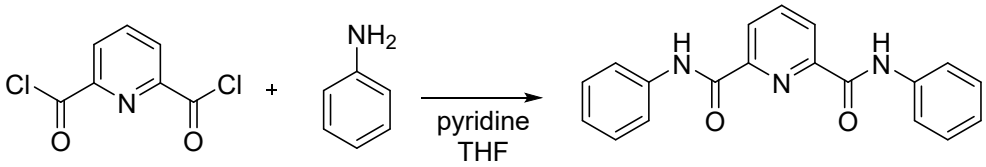

To an ice-cold solution of distilled aniline (140 µL, 1.5 mmol) in dry pyridine (1.5 mL) was gradually added to a solution of home-made pyridine 2,6-dicarbonyl chloride (150 mg, 0.74 mmol) in dry THF (5 mL). The reaction mixture was stirred at room temperature for 24h under Ar. The solvent was removed under reduced pressure, and the residue was rinsed thoroughly with water and saturated $Na_2CO_{3(aq)}$.(160 mg, 68%).

2. Tables

Table S1. Synthesis of CTF by using Dipicolinic acid and melamine under various reaction conditions.[a]

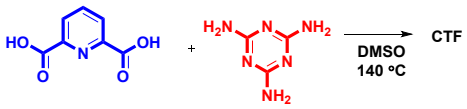

Entry	materials	Monomers	DMSO (mL)	Catalyst (mol%)	T (°C)	t (h)	CTF Yield (%)	S_{BET} (m^2g^{-1})	V_t (cm^3g^{-1})
1	-	DPA + Melamine	30	-	140	48	0	-	-
2	CTF-1	DPA + Melamine	10	-	140	48	35	100	0.75
3	Fe-CTF-2	DPA + Melamine	10	$FeCl_3$ (6)	140	48	55	245	1.85
4	Fe-CTF-3	DPA + Melamine	10	$FeCl_3$ (3)	140	48	73	683	1.34
5	Fe-CTF-4	DPA + Melamine	10	$FeCl_3$ (3)	140	24	44	348	2.26
6	-	DPA + Melamine	30	$FeCl_3$ (3)	140	48	0	-	-
7	-	DPA + Melamine	30	$FeCl_3$ (6)	140	48	0	-	-
8	-	DPA	10	$FeCl_3$ (3)	140	48	0	-	-

[a] reaction conditions: dipicolinic acid (0.835 g, 5 mmol) and melamine (0.427 g, 3.3 mmol) in the presence of $FeCl_3$ as catalyst and DMSO as solvent under described conditions.

Figures

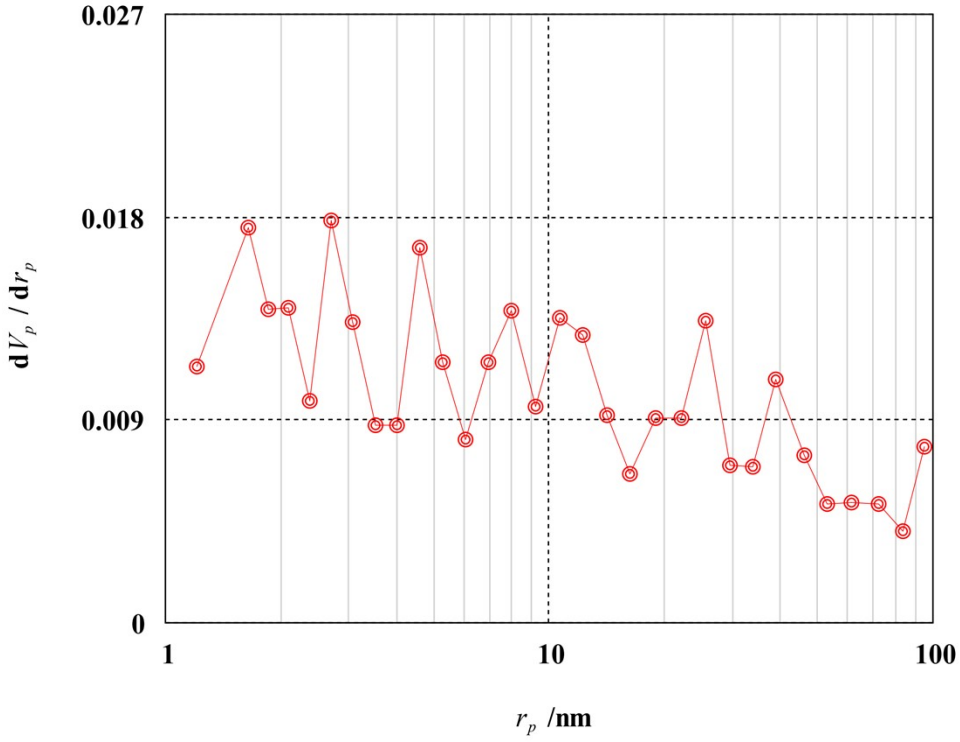

Figure S1. BJH pore size distribution for CTF-1. D_{BJH}= 5.4 nm.

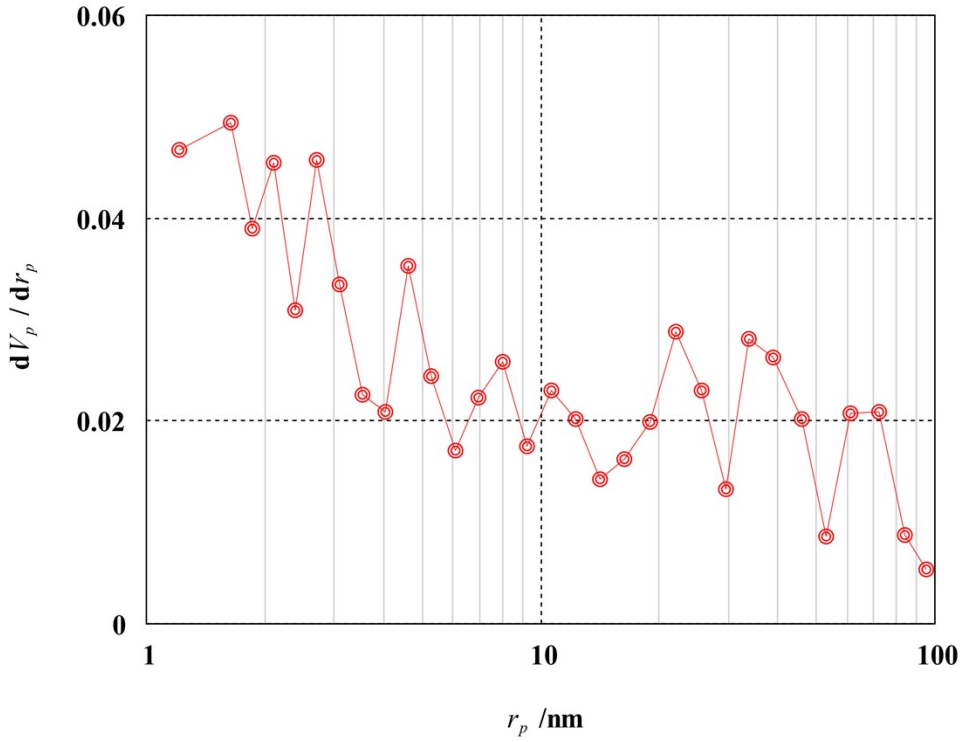

Figure S2. BJH pore size distribution for Fe-CTF-2. D_{BJH}= 3.2 nm.

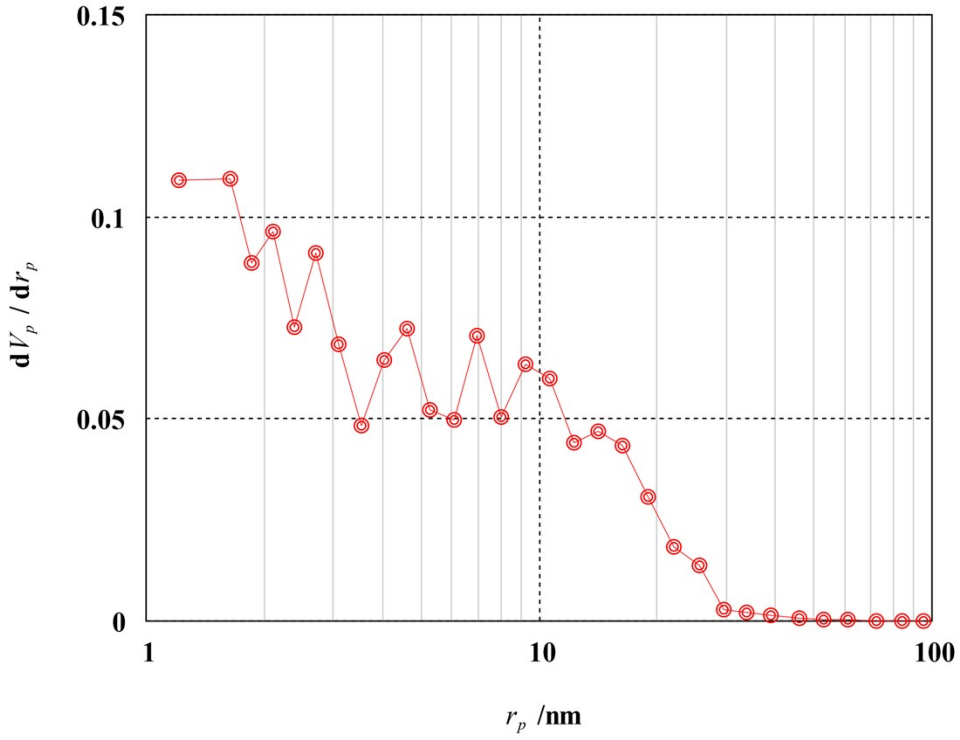

Figure S3. BJH pore size distribution for Fe-CTF-3. D_{BJH}= 3.2 nm.

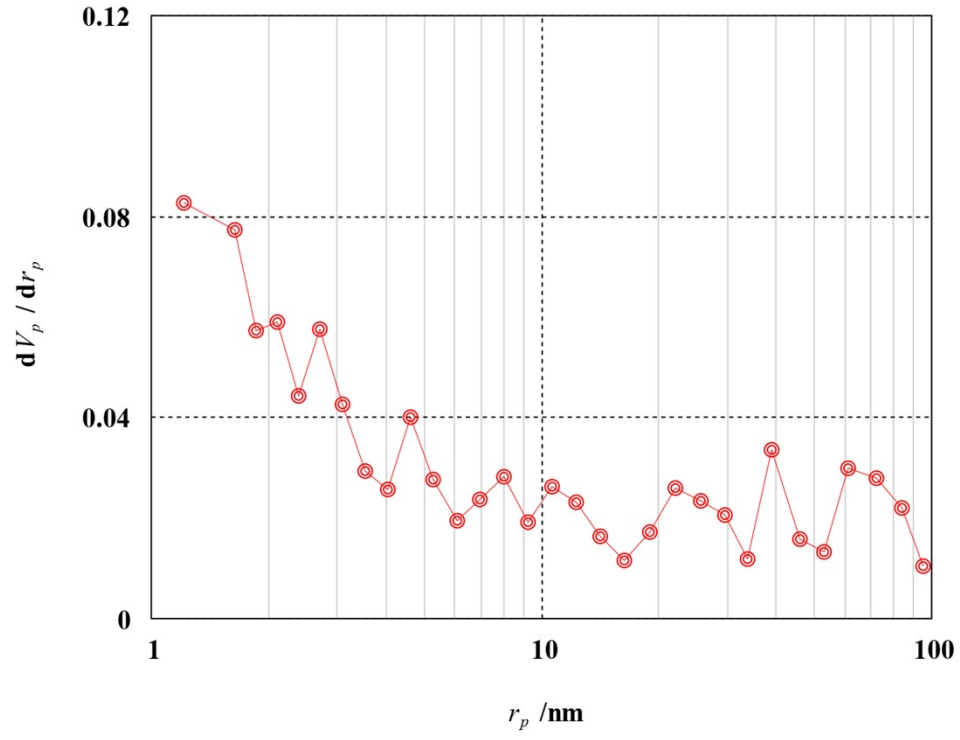

Figure S4. BJH pore size distribution for Fe-CTF-4. D_{BJH}= 2.4 nm.

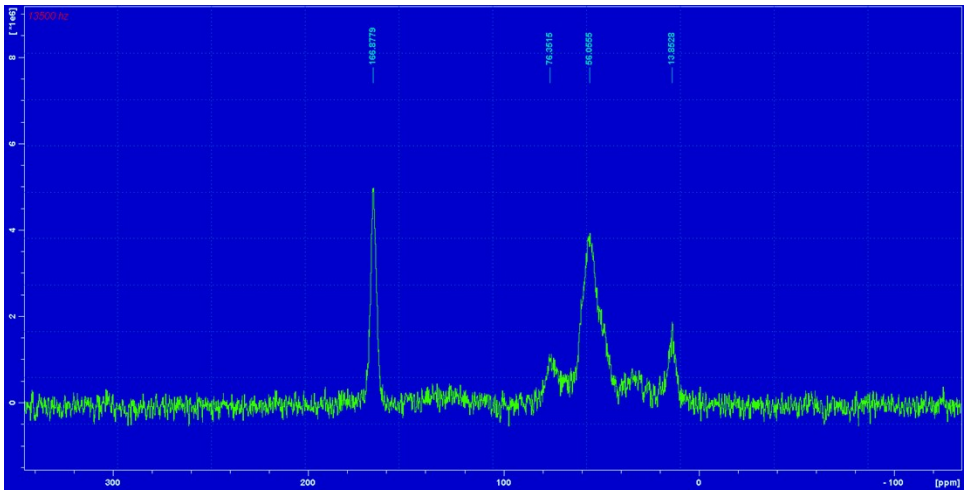

Figure S5. CP-MAS ^{13}C-NMR for Fe-CTF-2. Broad signals at δ 56 ppm (C–H) and δ 13 ppm (quaternary C) of the pyridine ring; the latter overlaps with the amidic C=O of dipicolinic acid. Assignments assume greater high-field paramagnetic shifting (Fe(III), low-spin, S = 1/2) for dipicolinic carbons than for triazine carbons.

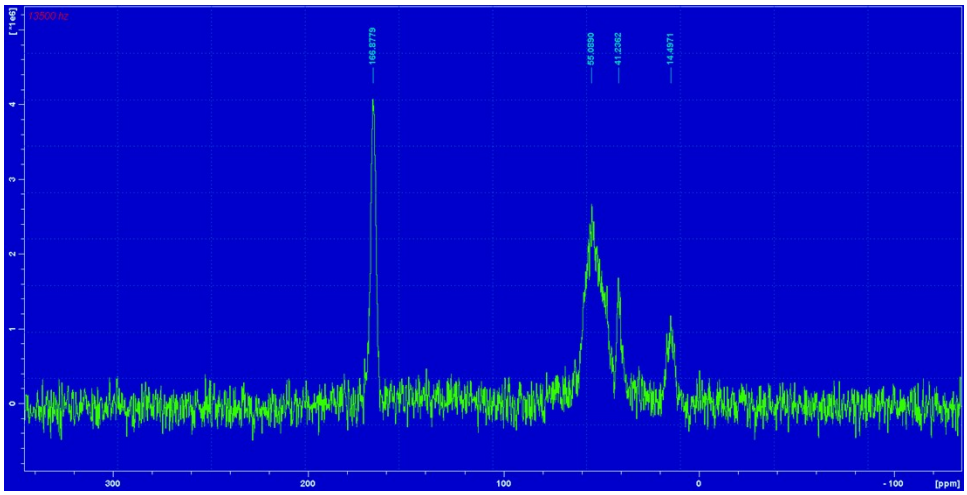

Figure S6. CP-MAS ^{13}C-NMR for Fe-CTF-4. Sharp peak at δ 165 ppm: triazine carbons. Broad signals at δ 55 ppm (pyridine C–H) and δ 14 ppm (pyridine quaternary C, overlapping with amidic C=O). Assignments assume greater high-field paramagnetic shift (Fe(III), S = 1/2) for dipicolinic vs. triazine carbons.

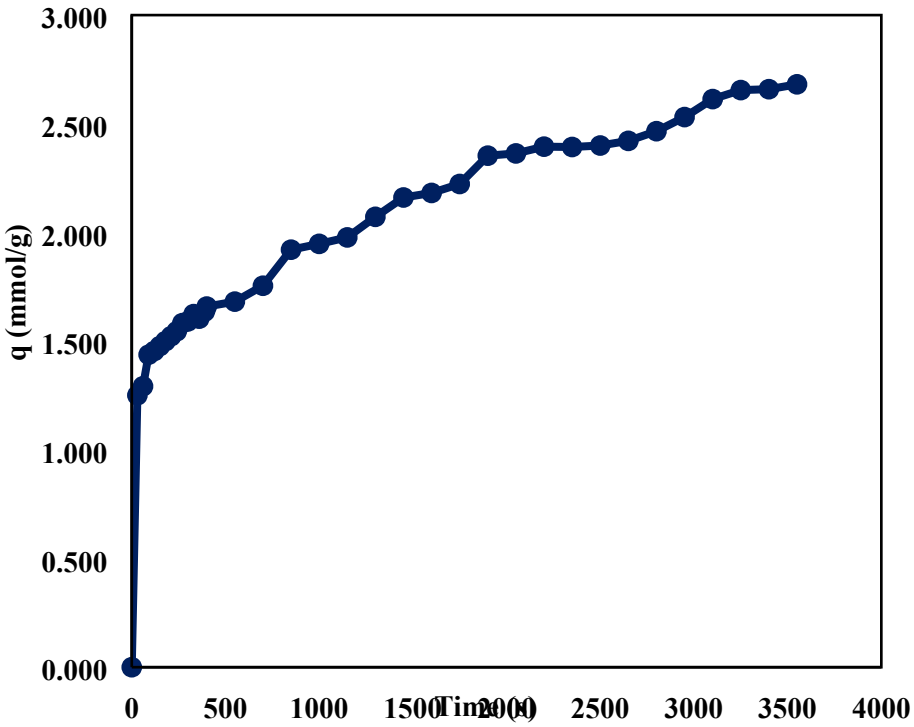

Figure S7. CO_2 adsorption capacity for Fe-CTF-3 (1 bar CO_2 at room temperature)

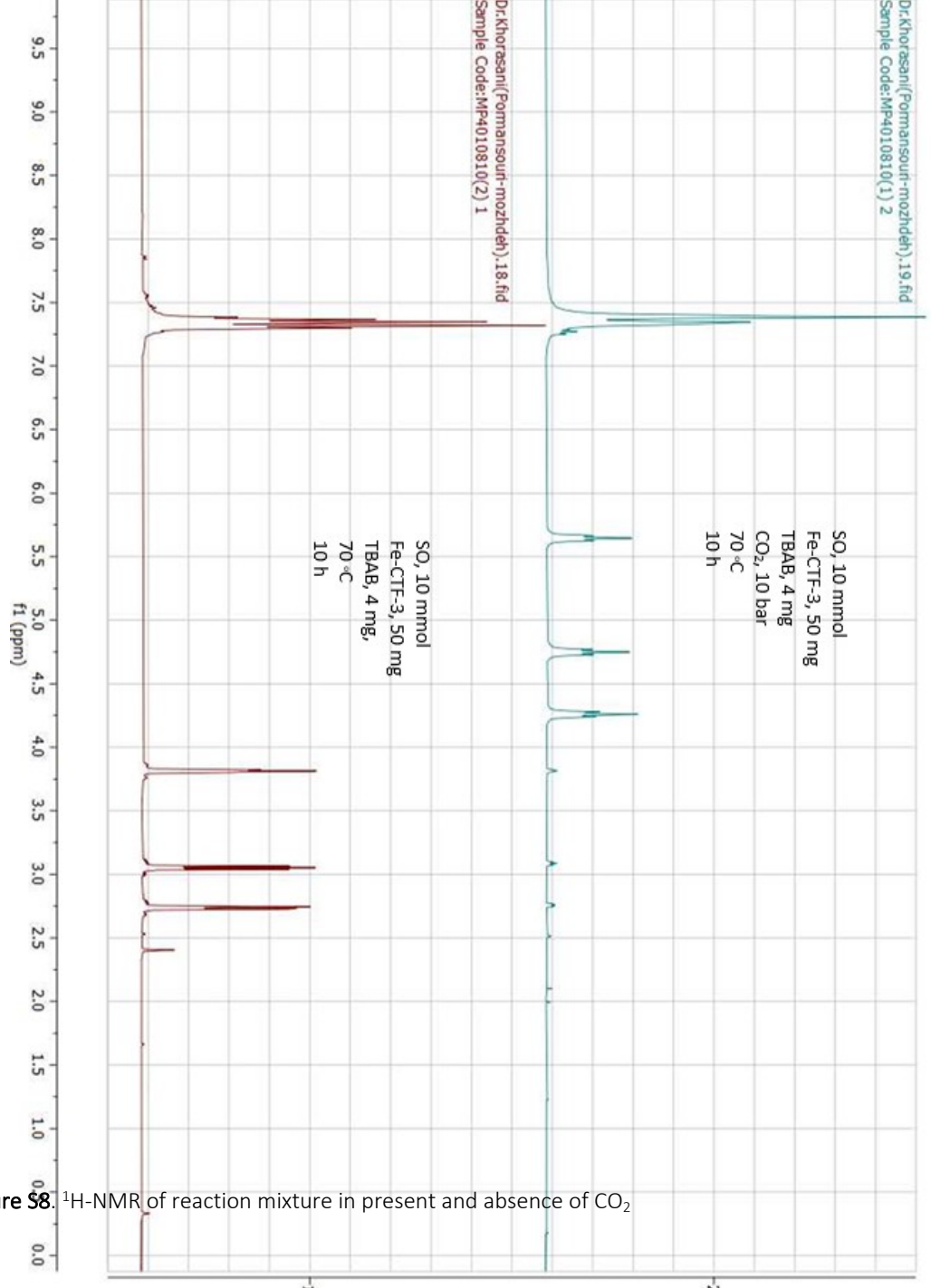

Figure S8. ^{1}H-NMR of reaction mixture in present and absence of CO_2

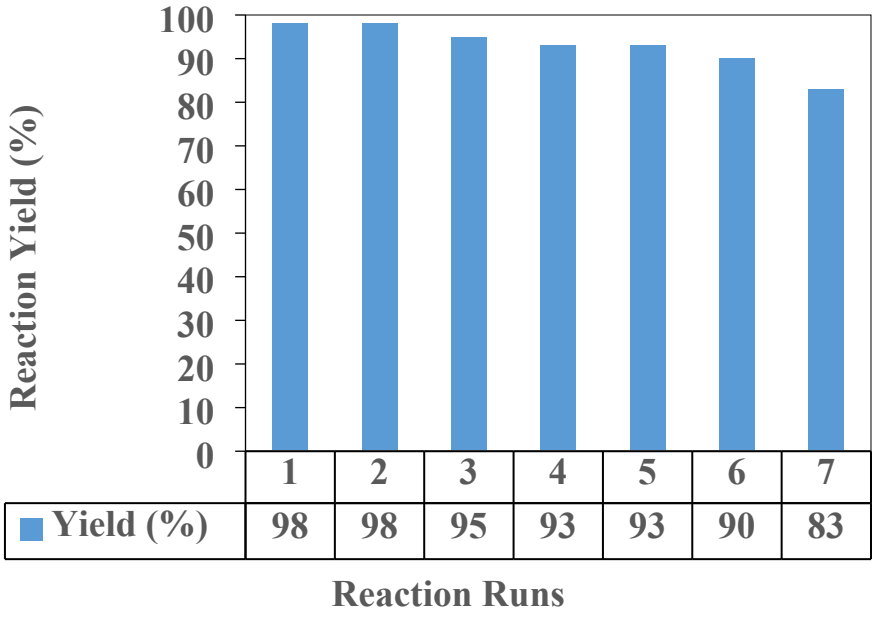

Figure S9. Reusability results for Fe-CTF-3. (reaction conditions: SO (10 mmol), Fe-CTF-3 (0.025 mol%). TBAB (0.125 mol%), CO_2 (10 bar) at 70 °C within 10 h.)

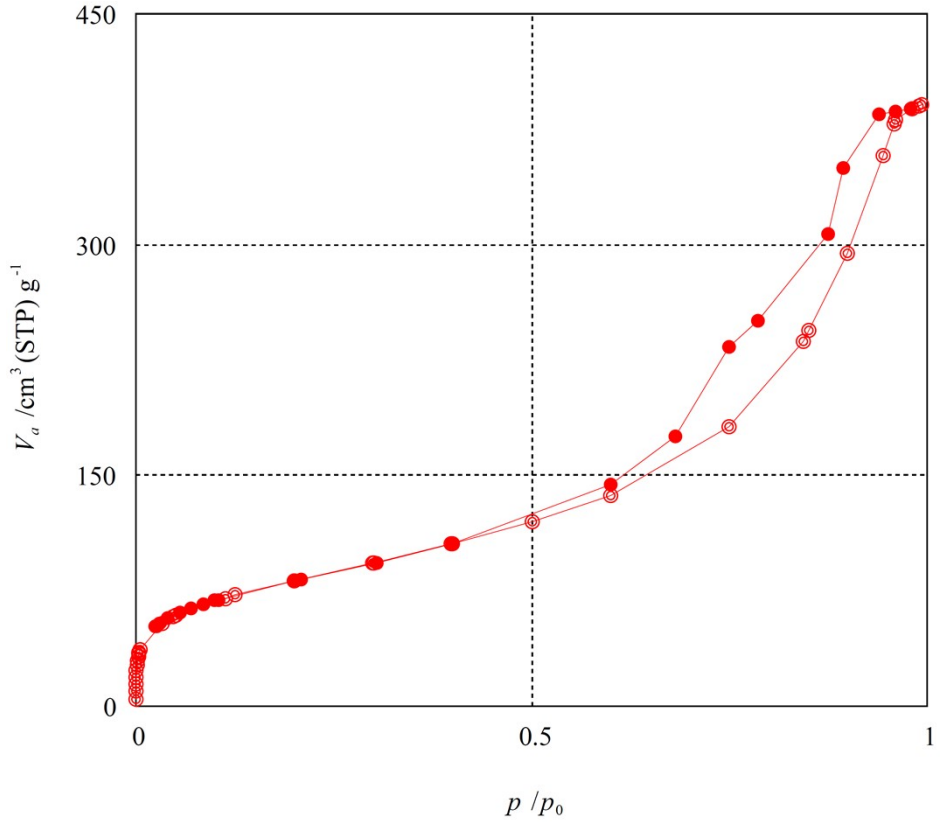

Figure S10. The nitrogen adsorption-desorption isotherm of recovered Fe-CTF-3. S_{BET}= 308 m^2 g^{-1}, V_t= 0.60 cm^3 g^{-1}.

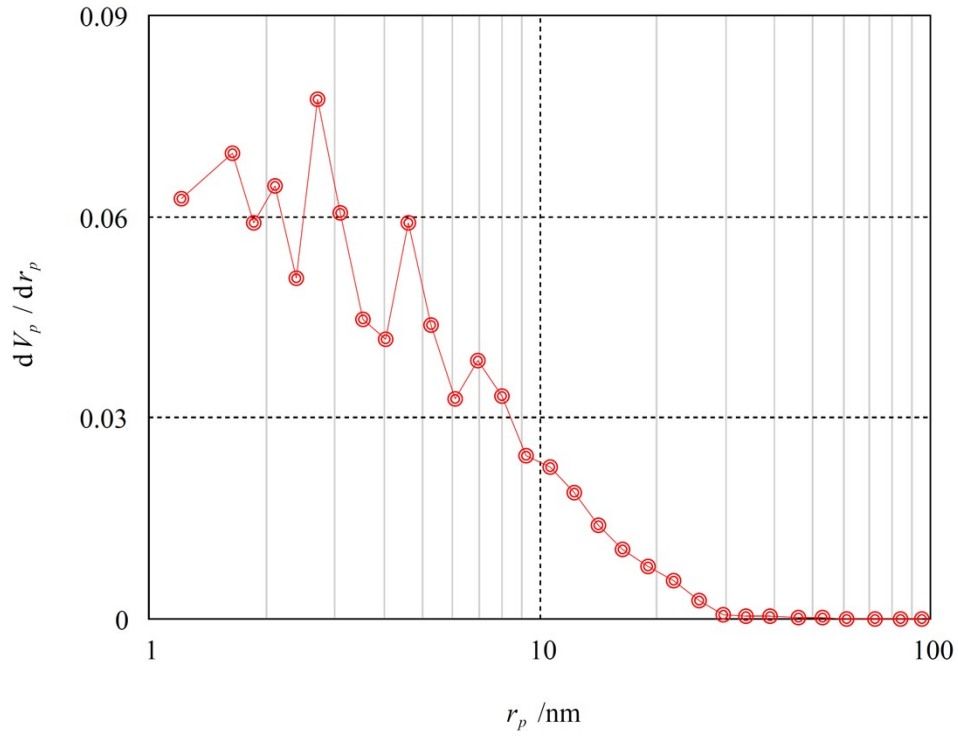

Figure S11. BJH pore size distribution for recovered Fe-CTF-3. D_{BJH}= 5.4 nm.

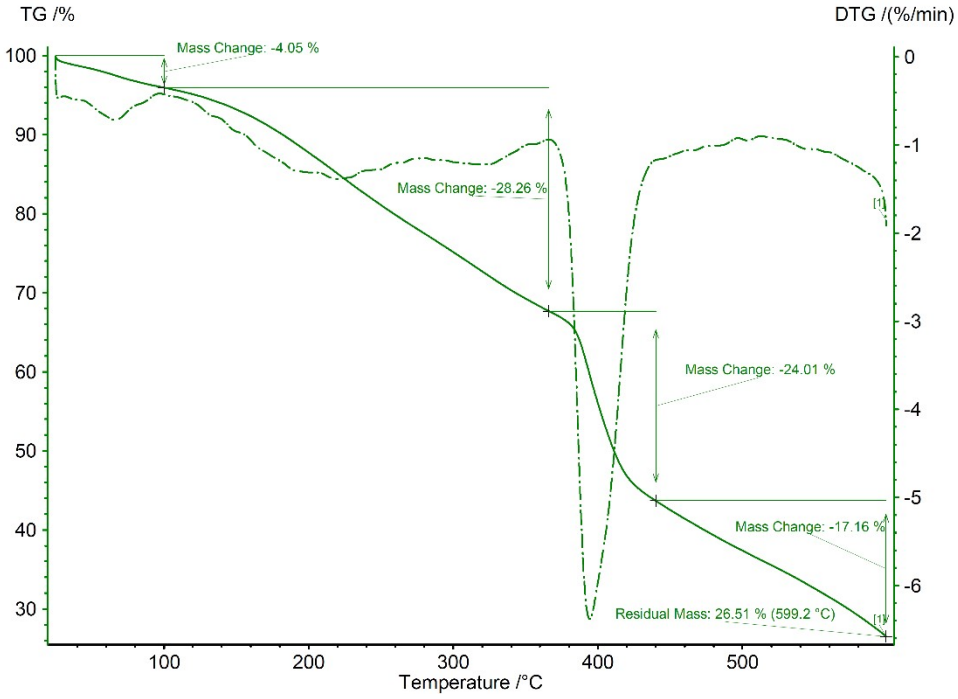

Figure S12. TG pattern for recovered Fe-CTF-3

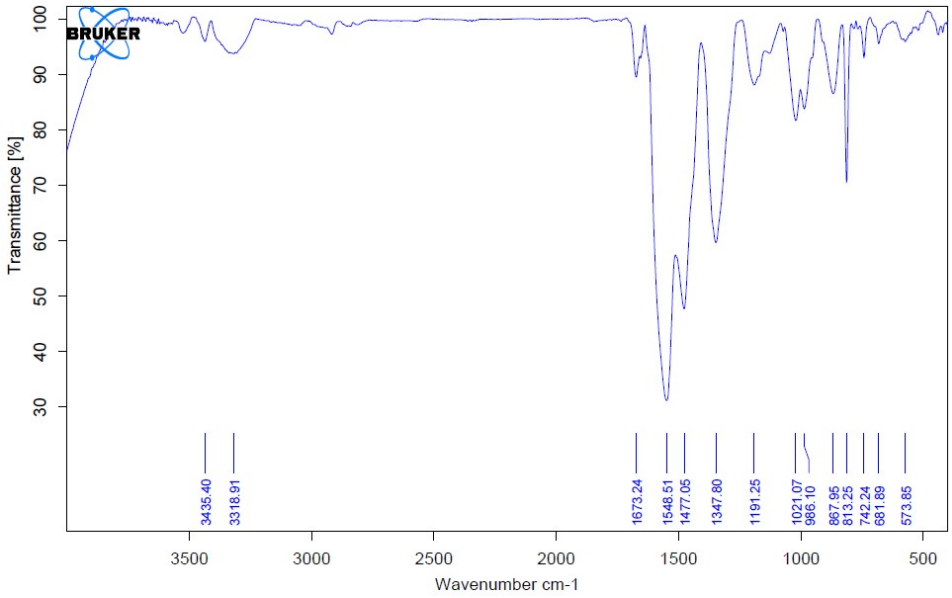

Figure S13. FTIR spectrum for recovered Fe-CTF-3

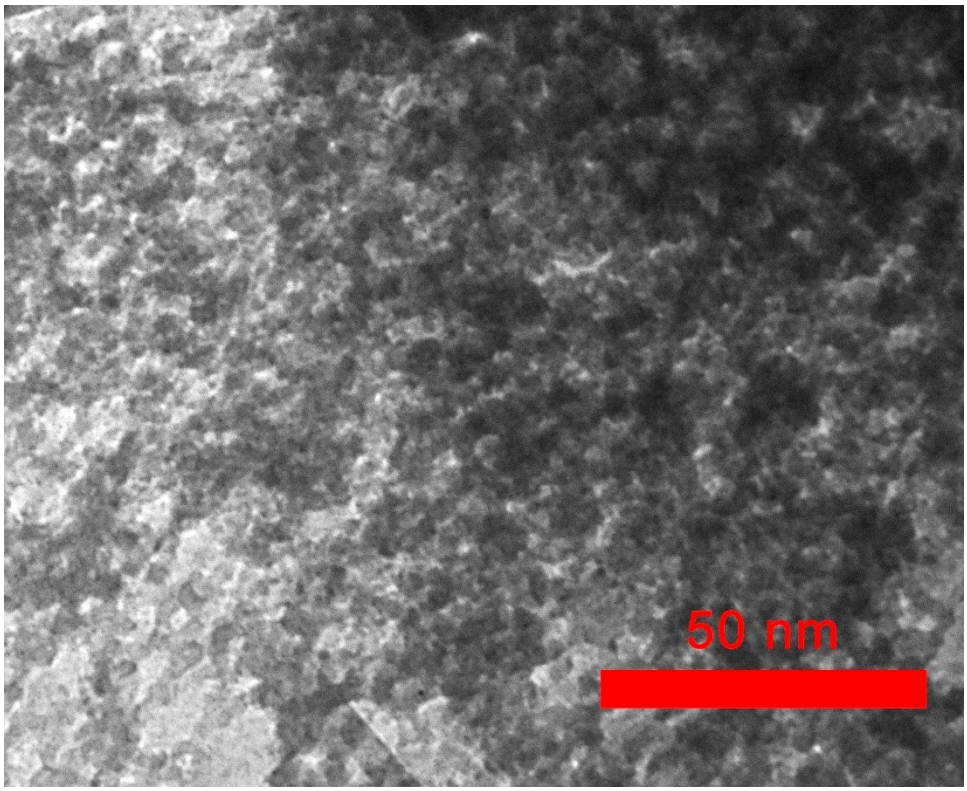

Figure S14. TEM image for recovered Fe-CTF-3

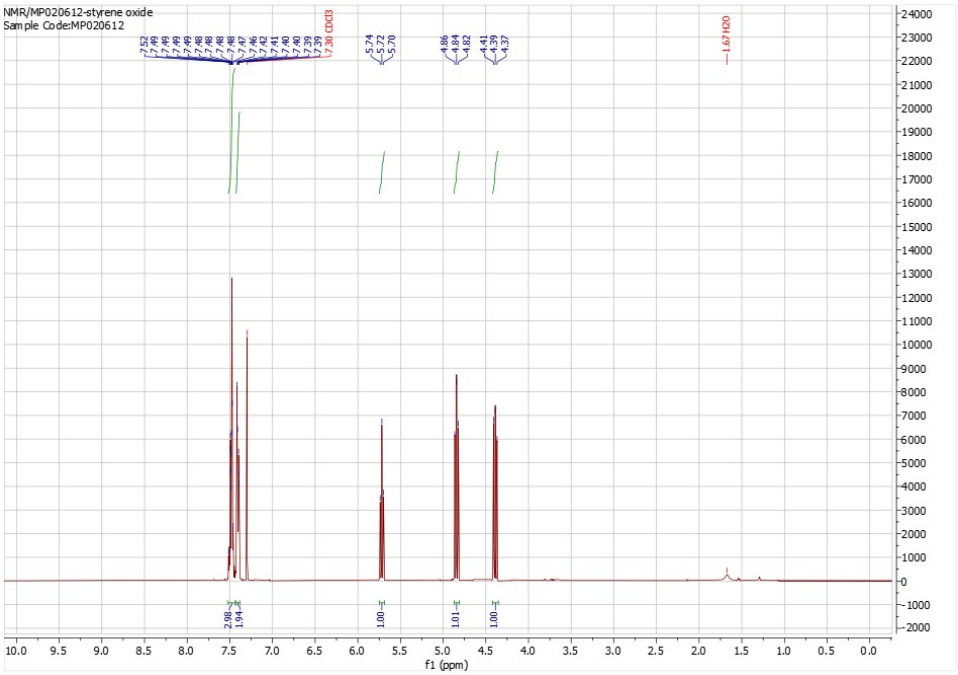

Figure S15. ^{1}H-NMR spectrum for styrene carbonate in $CDCl_3$ as solvent. ^{1}H-NMR (400 MHz, $CDCl_3$): δ(ppm) = 7.48-7.49 (m, 3H), 7.41 (d J= 8.0 Hz, 2H), 5.72 (t, *J*= 8.0 Hz, 1H), 4.82 (t, *J*= 8.0 Hz, 1H), 4.39 (t, *J*= 8.0 Hz, 1H).

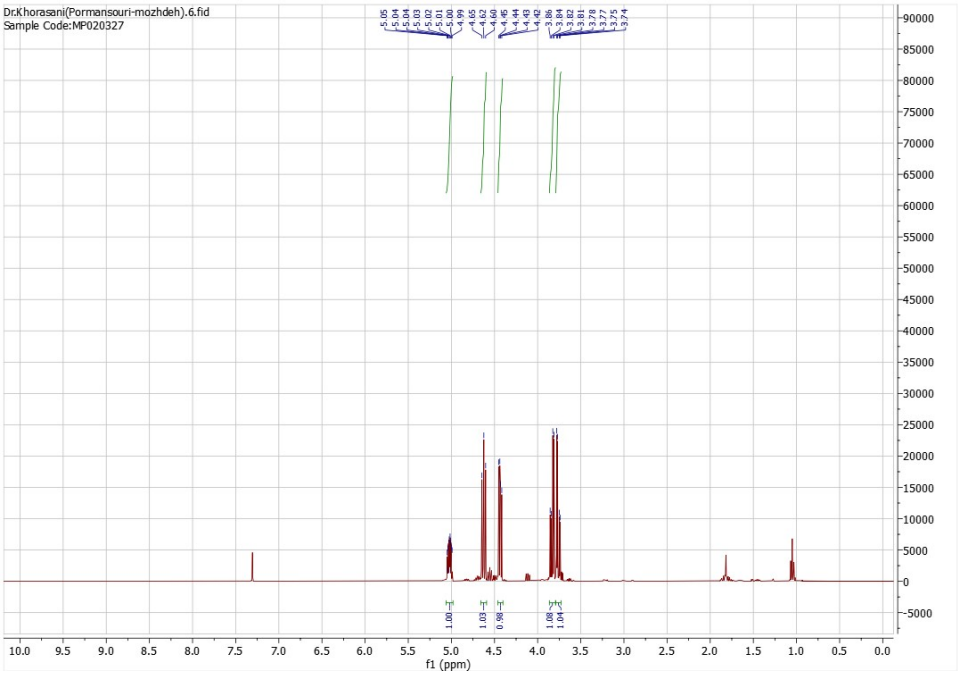

Figure S16. ^{1}H-NMR spectrum for epichlorohydrin carbonate in $CDCl_3$ as solvent. ^{1}H-NMR (400 MHz, $CDCl_3$): δ(ppm) = 4.99-5.05 (m, 1H), 4.62 (t, *J*= 8.0 Hz, 1H), 4.43 (dd, J_1= 8.0 Hz, J_2= 4.0 Hz, 1H), 3.82 (dd, J_1= 1.2 Hz, J_2= 4.0 Hz, 1H), 3.76 (dd, J_1= 1.2 Hz, J_2= 4.0 Hz, 1H).

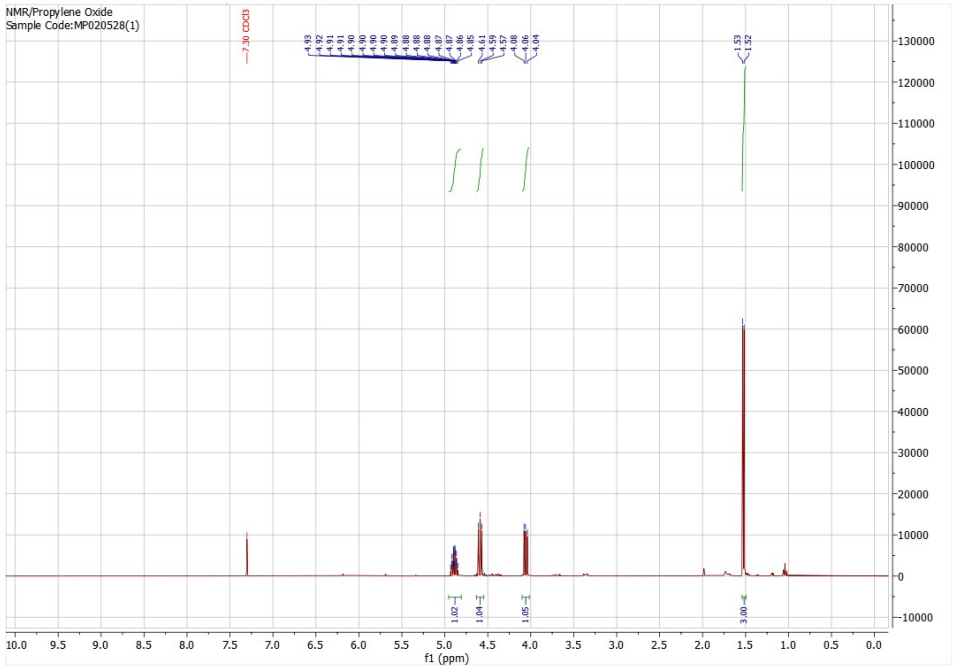

Figure S17. ^{1}H-NMR spectrum for propylene carbonate in $CDCl_3$ as solvent. ^{1}H-NMR (400 MHz, $CDCl_3$): δ(ppm) = 4.86-4.92 (m, 1H), 4.56 (t, *J*= 8.0 Hz, 1H), 4.06 (t, *J*= 8.0 Hz, 1H), 1.52 (d, *J*= 4.0 Hz, 3H).

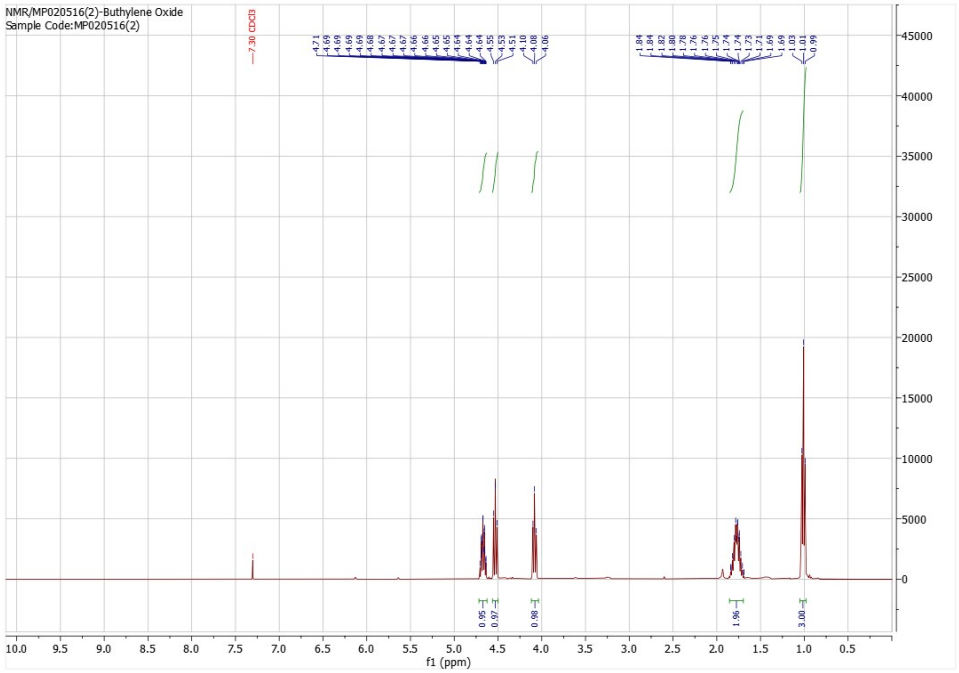

Figure S18. ^{1}H-NMR spectrum for butylene carbonate in $CDCl_3$ as solvent. ^{1}H-NMR (400 MHz, $CDCl_3$): δ(ppm) = 4.64-4.71 (m, 1H), 4.53 (t, *J*= 8.0 Hz, 1H), 4.08 (t, *J*= 8.0 Hz, 1H), 1.73-1.82 (m, 2H), 1.01 (t, *J*= 8.0 Hz, 3H).

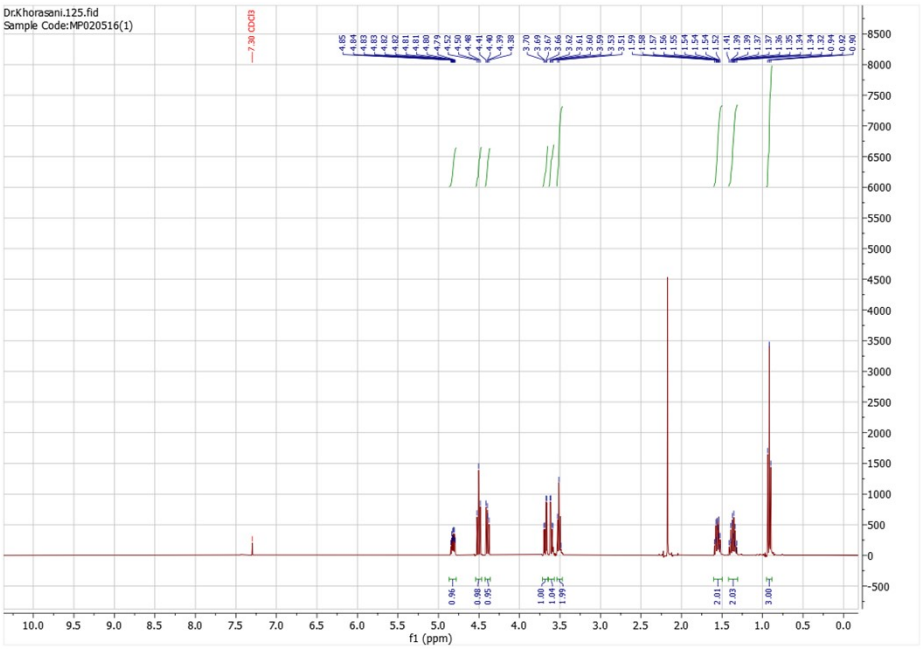

Figure S19. ^{1}H-NMR spectrum for butyl glycidyl carbonate in $CDCl_3$ as solvent. ^{1}H-NMR (400 MHz, $CDCl_3$): δ(ppm) = 4.79-4.85 (m, 1H), 4.50 (t, *J*= 8.0 Hz, 1H), 4.39 (dd, J_1= 8.0 Hz, J_2= 4.0 Hz, 1H), 3.67 (dd, J_1= 1.2 Hz, J_2= 4.0 Hz, 1H), 3.60 (dd, J_1= 1.2 Hz, J_2= 4.0 Hz, 1H), 3.51 (t, *J*= 8.0 Hz, 2H), 1.52-1.59 (m, 2H), 1.39-1.42 (m, 2H), 0.92 (t, *J*= 8.0 Hz, 3H).

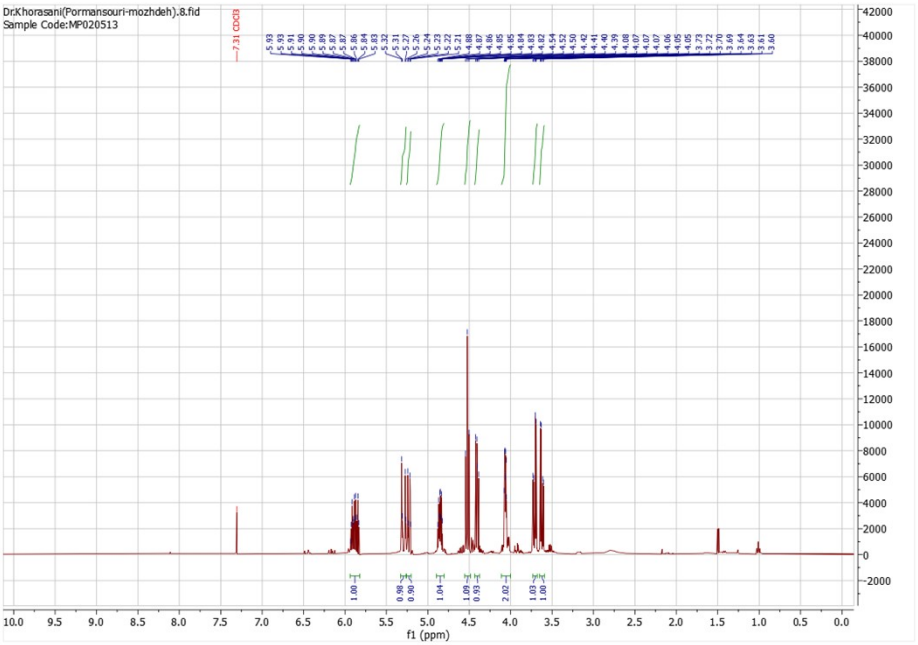

Figure S20. ^{1}H-NMR spectrum for allyl glycidyl carbonate in $CDCl_3$ as solvent. ^{1}H-NMR (400 MHz, $CDCl_3$): δ(ppm) = 5.83-5.93 (m, 1H), 5.29 (dd, J_1= 20.0 Hz, J_2= 4.0 Hz, 1H), 5.22 (dd, J_1= 0.0 Hz, J_2= 4.0 Hz, 1H), 4.82-4.88 (m, 1H), 4.52 (t, *J*= 8.0 Hz, 1H), 4.40 (dd, J_1= 8.0 Hz, J_2= 4.0 Hz, 1H), 4.05-4.08 (m, 2H), 3.71 (dd, J_1= 1.2 Hz, J_2= 4.0 Hz, 1H), 3.62 (dd, J_1= 1.2 Hz, J_2= 4.0 Hz, 1H).

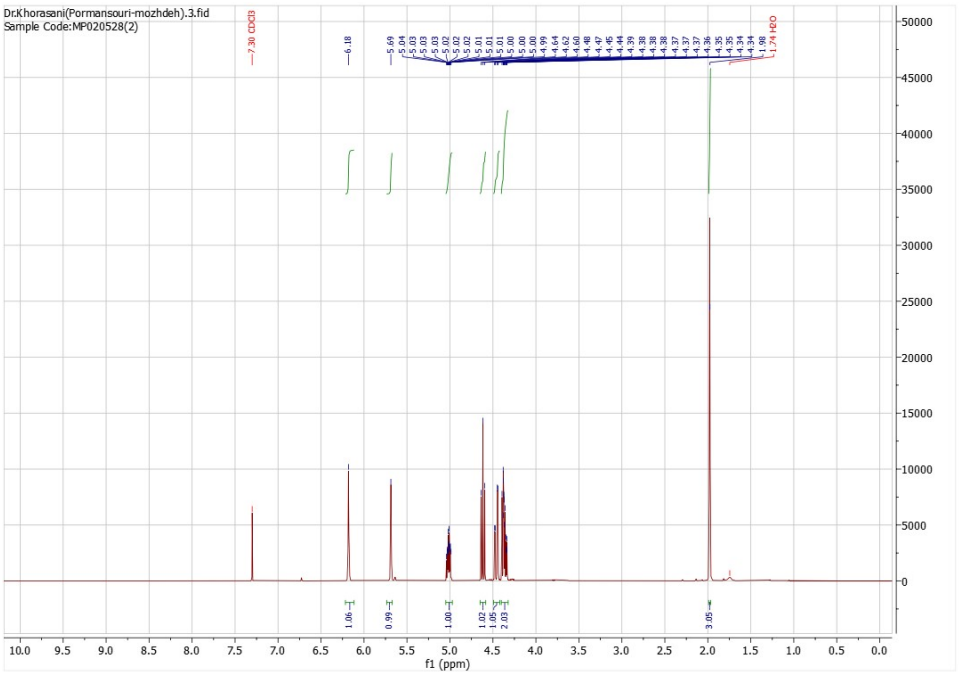

Figure S21. ^{1}H-NMR spectrum for methylmetaacrylate glycidyl carbonate in $CDCl_3$ as solvent. ^{1}H-NMR (400 MHz, $CDCl_3$): δ(ppm) = 6.18 (s, 1H), 5.69 (s, 1H), 4.99-5.04 (m, 1H), 4.62 (t, *J*= 8.0 Hz, 1H), 4.46 (dd, J_1= 1.2 Hz, J_2= 4.0 Hz, 1H), 4.34-4.39 (m, 2H), 1.98 (s, 3H).

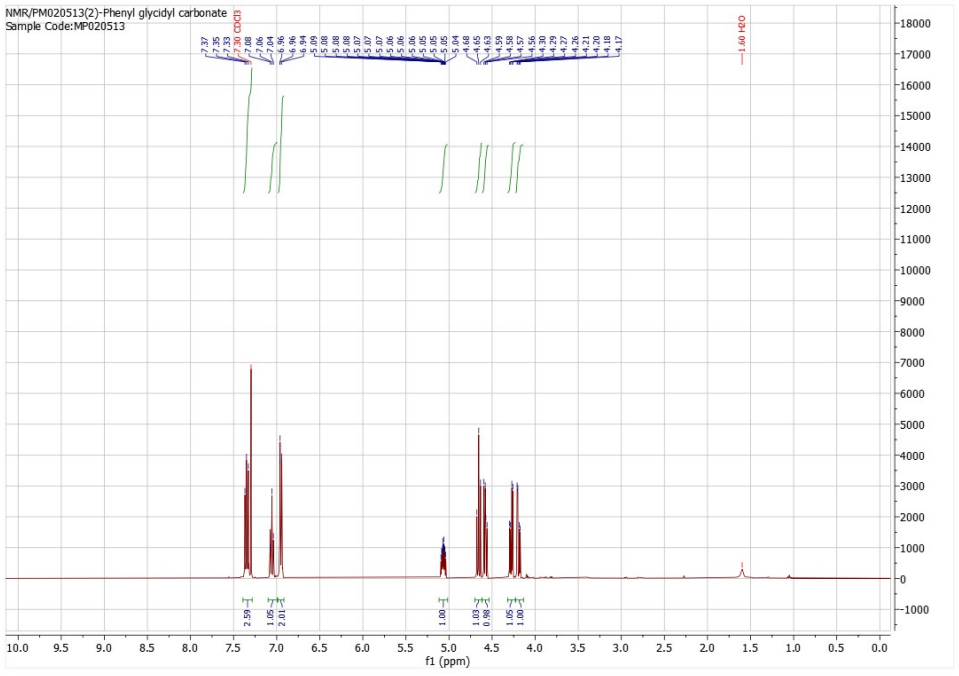

Figure S22. ^{1}H-NMR spectrum for phenyl glycidyl carbonate in $CDCl_3$ as solvent. ^{1}H-NMR (400 MHz, $CDCl_3$): δ(ppm) = 7.35 (t, *J*= 8.0 Hz, 2H), 7.06 (t, *J*= 8.0 Hz, 1H), 6.96 (d, *J*= 8.0 Hz, 2H), 5.04-5.09 (m, 1H), 4.63 (t, *J*= 8.0 Hz, 1H), 4.57 (dd, J_1= 8.0 Hz, J_2= 4.0 Hz, 1H), 4.28 (dd, J_1= 1.2 Hz, J_2= 4.0 Hz, 1H), 4.19 (dd, J_1= 1.2 Hz, J_2= 4.0 Hz, 1H).

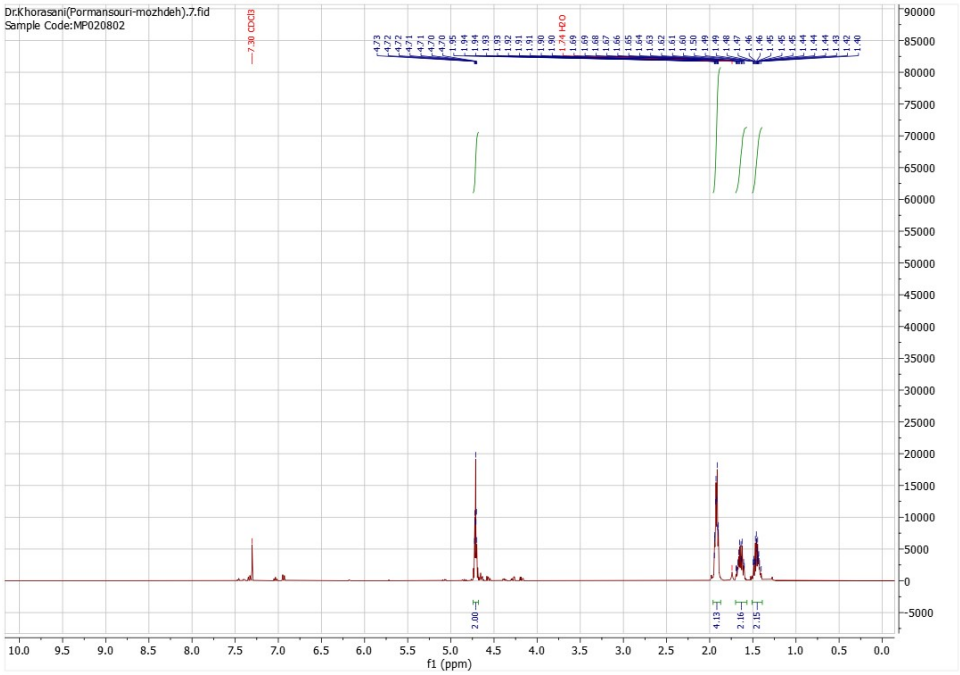

Figure S23. ^{1}H-NMR spectrum for cyclohexene carbonate in $CDCl_3$ as solvent. ^{1}H-NMR (400 MHz, $CDCl_3$): δ(ppm) = 4.70-4.73 (m, 2H), 1.90-1.95 (m, 4H), 1.60-1.69 (m, 2H), 1.40-1.50 (m, 2H).

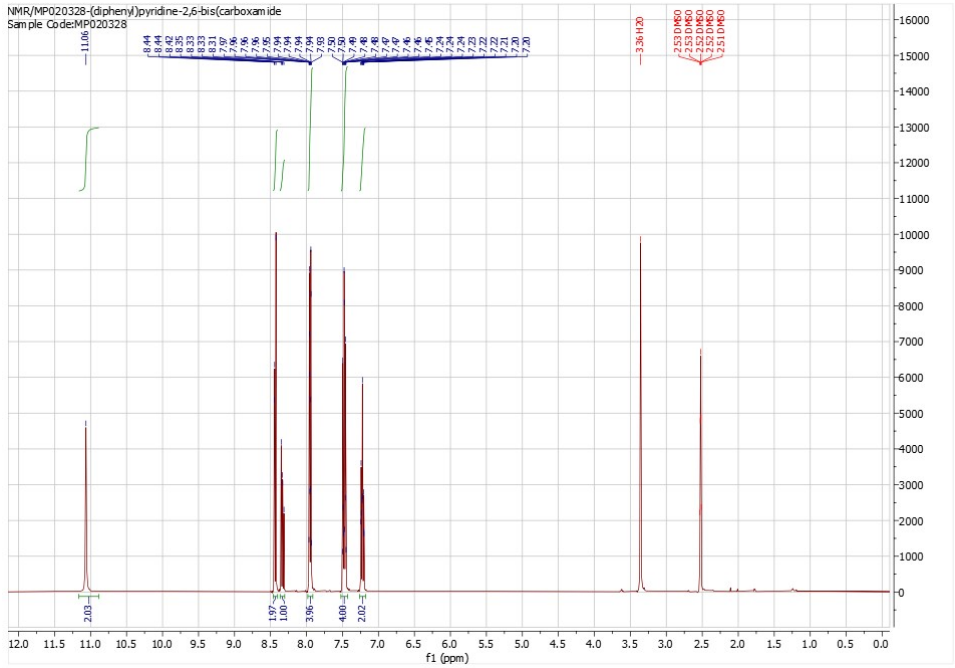

Figure S24. ^{1}H-NMR spectrum for N^2,N^6-diphenylpyridine-2,6-dicarboxamide (denoted as monomer) in DMSO-d_6 as solvent. ^{1}H-NMR (400 MHz, DMSO-d_6): δ(ppm) = 11.06 (s, 2H), 8.43 (d, *J*= 8.0 Hz, 2H), 8.33 (t, *J*= 8.0 Hz, 1H), 7.95 (d, *J*= 8.0 Hz, 4H), 7.48 (t, *J*= 8.0 Hz, 4H), 7.22 (t, *J*= 8.0 Hz, 2H).

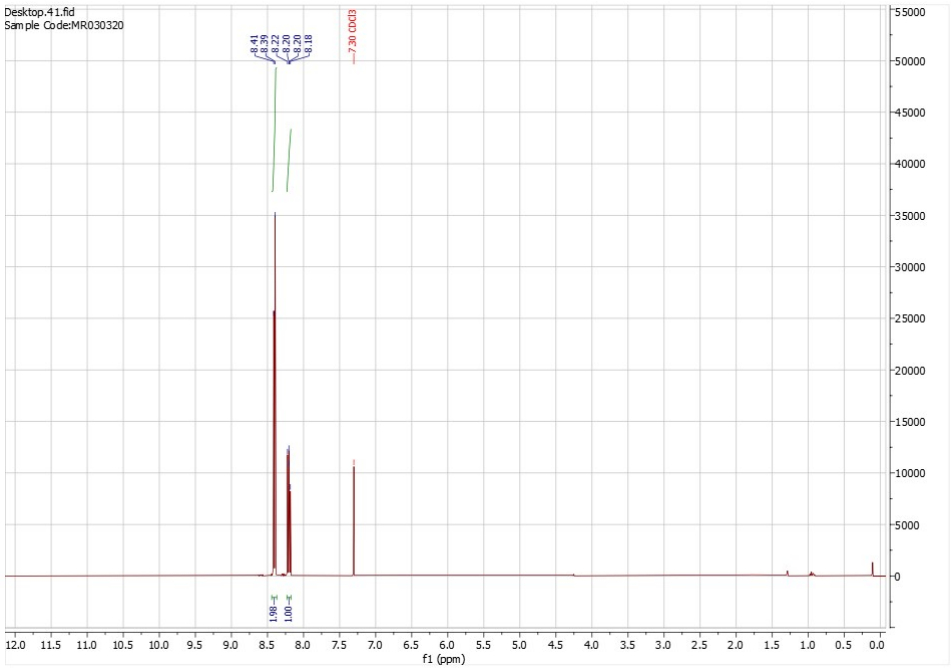

Figure S25. ^{1}H-NMR spectrum for pyridine-2,6-dicarbonyl chloride in $CDCl_3$ as solvent. ^{1}H-NMR (400 MHz, $CDCl_3$): δ(ppm) = 8.40 (d, *J*= 8.0 Hz, 2H), 8.20 (t, *J*= 8.0 Hz, 1H).

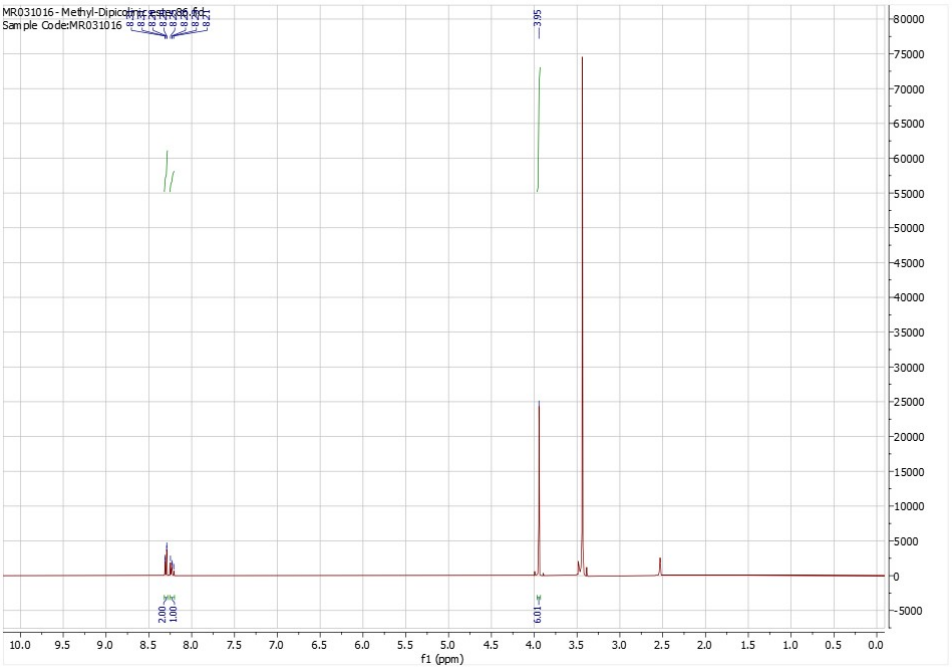

Figure S26. ^{1}H-NMR spectrum for dimethyl pyridine-2,6-dicarboxylate in DMSO-d_6 as solvent. ^{1}H-NMR (400 MHz, DMSO-d_6): δ(ppm) = 8.30 (d, *J*= 8.0 Hz, 2H), 8.20 (t, *J*= 8.0 Hz, 1H), 3.95 (s, 6H).